Conditions for efficient and stable ion acceleration by moderate circularly polarized laser pulses at intensities of 1020 W/cm2

B. Qiao, M. Zepf, P. Gibbon, M. Borghesi, B. Dromey et al.

Citation: Phys. Plasmas **18**, 043102 (2011); doi: 10.1063/1.3577573
View online: http://dx.doi.org/10.1063/1.3577573
View Table of Contents: http://pop.aip.org/resource/1/PHPAEN/v18/i4
Published by the American Institute of Physics.

Conditions for efficient and stable ion acceleration by moderate circularly polarized laser pulses at intensities of 10^{20} W/cm^2

B. Qiao,[1,2,a)] M. Zepf,[1] P. Gibbon,[2] M. Borghesi,[1] B. Dromey,[1] S. Kar,[1] J. Schreiber,[3] and M. Geissler[1]
[1]*School of Mathematics and Physics, Queen's University Belfast, Belfast BT7 1NN, United Kingdom*
[2]*Jülich Supercomputing Center, Forschungzentrum Jülich GmbH, D-52425 Jülich, Germany*
[3]*Max-Planck-Institut für Quantenoptik, D-85748 Garching, Germany*

(Received 1 February 2011; accepted 22 March 2011; published online 20 April 2011)

Conditions for efficient and stable ion radiation pressure acceleration (RPA) from thin foils by circularly polarized laser pulses at moderate intensities are theoretically and numerically investigated. It is found that the unavoidable decompression of the co-moving electron layer in Light-Sail RPA leads to a change of the local electrostatic field from a "bunching" to a "debunching" profile, ultimately resulting in premature termination of ion acceleration. One way to overcome this instability is the use of a multispecies foil where the high-Z ions act as a sacrificial species to supply excess co-moving electrons for preserving stable acceleration of the lower-Z ion species. It is shown by 2D particle-in-cell simulations that 100 MeV/u monoenergetic C^{6+} ion beams are produced by irradiation of a Cu–C-mixed foil with laser pulses at intensities 5×10^{20} W/cm^2, which can be easily achieved by current day lasers. © *2011 American Institute of Physics*. [doi:10.1063/1.3577573]

I. INTRODUCTION

Ion acceleration from laser-irradiated solid foils has been extensively studied over the past few years.[1–9] High-quality ion beams have many prospective applications[5] including medical isotope production, tumor therapy, ultrafast radiography, and laser-driven fusion. Theoretical models and simulations based on one-dimensional (1D) geometry have shown that radiation pressure acceleration (RPA)[3,6,7] using circularly polarized (CP) laser pulses may be a promising route to obtaining high-quality monoenergetic ion beams in a much more efficient manner, compared to the target normal sheath acceleration (TNSA).[1,4] It has been predicted by 1D particle-in-cell (PIC) simulations that CP laser pulses can produce hundreds of MeV monoenergetic proton beams via quasistable RPA. The key effect of CP is the absence of the oscillating $\mathbf{j} \times \mathbf{B}$ force which suppresses the heating and subsequent circulation of electrons through the foil.

In a more realistic multidimensional geometry, unfortunately the acceleration cannot be as stable as predicted by 1D simulations.[6] The accelerating ion beam debunches quickly, resulting in reduced maximum energy and broadened spectrum. It has been generally believed that the transverse instability because of nonuniform laser irradiation leads to rapid foil deformation and premature termination of ion acceleration. This transverse instability has been explained by various names, such as "Rayleigh-Taylor-like"[10] and "surface-instability."[11] Several schemes[11,12] using either special high-order Gaussian laser modes or complicated target shaping and multispecies to suppress these instabilities have been claimed. A recent paper[13] has demonstrated stable GeV proton acceleration from a double-layer foil target irradiated by ultraintense lasers at intensities of 3.9×10^{22} W/cm^2. However, all these schemes have been investigated in simulations using very high-intensity lasers of $I_0 \geq 10^{22}$ W/cm^2 ($a \geq 100$). For such ultraintense lasers, it has been shown[8] that the whole plasma slab including electrons and ions is rapidly accelerated to relativistic energies $(\gamma - 1)m_i c^2$ in initial hole-boring (HB) phase within a very short time. During the subsequent "Light-Sail" (LS) phase any instabilities are much suppressed as their growth rate becomes γ times slower in the slab-moving frame. In the limit of extremely high intensities 10^{23} W/cm^2, where relativistic energies are achieved within one laser cycle, Esirkepov *et al.*[2] showed that stable acceleration of the foil central focal region can be achieved using linearly polarized lasers with Gaussian focal shape and uniform foils. It has been also found[9] that stable RPA can be achieved using sub-skin-depth nanofoils in a new Leaky LS regime, where 100 MeV proton beams of comparatively low densities are obtained. Unfortunately, either such ultraintense lasers of 10^{22} W/cm^2 or ultrathin nanofoils are very difficult to be achieved in experiments so far.

While focal spot/foil shaping and the use of CP extends the regime of stable acceleration to a wider parameter range they are clearly not sufficient criteria. Nor do they explain what the key criterion for stable foil acceleration is, in particular that for the case of moderate laser intensities. In this paper, we reexamine ion RPA in more realistic multidimensional geometry through theoretical modeling and PIC simulations. It is found that stable acceleration of the ion beam depends critically on whether the latter can remain accompanied with enough co-moving electrons during the acceleration, because only locally negative (or quasineutral) charge space can preserve a bunching (uniform) profile of the electrostatic field thus allowing ions to be synchronously accelerated with a narrow energy spread. Generally speaking, in the LS RPA regime the electron layer undergoes unavoidable

a)Electronic mail: b.qiao@qub.ac.uk.

decompression because the Debye length of the hot plasma slab $\lambda_D = kT/4\pi n_e e^2$ is larger than its thickness, where T and n_e are electron temperature and density, respectively. Furthermore, this decompression is much accelerated in multidimensional case by the enhanced electron heating due to the transverse instabilities. The decompression of the co-moving electrons leads to a change of the local electrostatic field on the ion beams from a bunching to a debunching profile, resulting in premature termination of the acceleration. Based on this, a possible scheme to achieve efficient and stable ion RPA by moderate CP laser pulses is proposed using a multispecies foil. In the scheme, the high-charge-state (Z_{i1}) ions act as a sacrificial species to supply excess co-moving electrons for preserving stable RPA of the lower-Z_{i2} ion species. It is shown by 2D PIC simulations that high-density 100 MeV/u monoenergetic C^{6+} ion beams are produced by irradiation of a copper–carbon-mixed (Cu–C-mixed) foil with CP laser pulses at moderate intensities of 5×10^{20} W/cm^2, which are easily achievable by current day lasers.

II. THEORETICAL MODEL OF REALISTIC RPA SCHEME

A. Key conditions for stable RPA

We start from the original RPA model shown in schematic Fig. 1(a). In the ideal case, a plasma slab including both ion and electron layers is synchronously accelerated by laser pulses as a mirror. However, unlike the acceleration of a cold mirror at low light intensities, in high-intensity regime the laser ponderomotive pressure acts on the electrons and is then mediated to the ions via the electrostatic field E_z within the slab [see Fig. 1(a)]. A simple theoretical model can be given for acceleration of these ions in the slab. We assume an ion beam of thickness l, density n_i, and charge state Z_i is pushed along z-axis with the co-moving electron density n_e. According to the Gauss law $\nabla \cdot \mathbf{E} = 4\pi\rho = 4\pi(n_i q_i - n_e e)$, the local electrostatic field E_z acting on the ion beam satisfies

$$\frac{\partial E_z}{\partial z} = 4\pi e(n_i Z_i - n_e) = \begin{cases} -\kappa < 0 & \text{if } n_e > n_i Z_i \\ \kappa > 0 & \text{if } n_e < n_i Z_i, \end{cases} \quad (1)$$

where $q_i = n_i Z_i e$ and κ is a positive constant. If assuming E_z has a linear profile,[3,14] we obtain that $E_z = E_0/2 \mp \kappa(z_i - z_c)$, where $z_c = z_0 + l/2$ is the mass central of the ion beam and $z_0 < z_i < z_0 + l$, $E_0 = (8\pi I/c)^{1/2}$, equivalent to the laser radiation pressure.

Ions at the position z_i within the ion beam are accelerated by the local $E_z(z_i)$, whose motions obey

$$\frac{d^2 z_i}{dt^2} = \frac{q_i}{2m_i\gamma_i^3} E_0 \mp \frac{q_i}{m_i\gamma_i^3} \cdot \kappa(z_i - z_c). \quad (2)$$

Introducing $\xi = z_i - z_c$ to represent ion relative position to the beam mass central and assuming $\gamma_i \approx \gamma_0$, from Eq. (2) we obtain that

$$\frac{d^2 z_c}{dt^2} = \frac{1}{2}\alpha E_0 = \frac{1}{2}\alpha\sqrt{\frac{8\pi I}{c}}, \quad (3)$$

$$\frac{d^2\xi}{dt^2} = \begin{cases} -\alpha\kappa\xi & \text{if } n_e > n_i Z_i, \quad (4a) \\ \alpha\kappa\xi & \text{if } n_e < n_i Z_i, \quad (4b) \end{cases}$$

where $\alpha = q_i/m_i\gamma_0^3$. We see that all ions of the ion beam as a whole are accelerated by the laser radiation pressure [Eq. (3)], while in the boosted frame their individual motions are determined by Eq. (4a) or (4b), depending on the local charge density.

In the ideal RPA model, as an additional consequence of the piling up of electrons in the initial HB phase [Fig. 1(a1)], the plasma slab is negatively charged due to excess electrons ($n_e > n_i Z_i$). When E_z has a negative gradient $E_z = E_0/2 - \kappa(z_i - z_c)$ [Fig. 1(a2)], the ion phase motion (ξ, t) [Eq. (4a)] is a harmonic oscillation $\xi = \xi_0 \cos(\alpha\kappa t)$. This indicates that the faster ions experience a smaller accelerating field, and the slower ions a larger field, resulting in the well-known "rolled-up" phase space of RPA[3,6,7] and consequently in a high-density monoenergetic ion beam synchronously accelerated by the laser. We refer to such $E_z = E_0/2 - \kappa(z_i - z_c)$ [Fig. 1(a2)] as the bunching electric field.

In 1D simulations, the co-moving electron layer decompresses very slowly due to the fact that the electrons remain at a low temperature in 1D case such that the Debye length is short compared to the slab thickness. This ensures that only a small fraction of the ion beam at the laser-facing side experiences a debunching field and the major part is quasistably accelerated by the bunching profile of E_z [see Fig. 1(b1)], resulting in a typical phase space structure seen in 1D simulations:[3,6,7] a distinct "head" with the majority of concentrated ions and a long "tail" with a very low amount of trailing ions.

However, in a more realistic (multidimensional) case, the electrons in the plasma slab are heated far more substantially than in 1D simulations resulting in a Debye length that

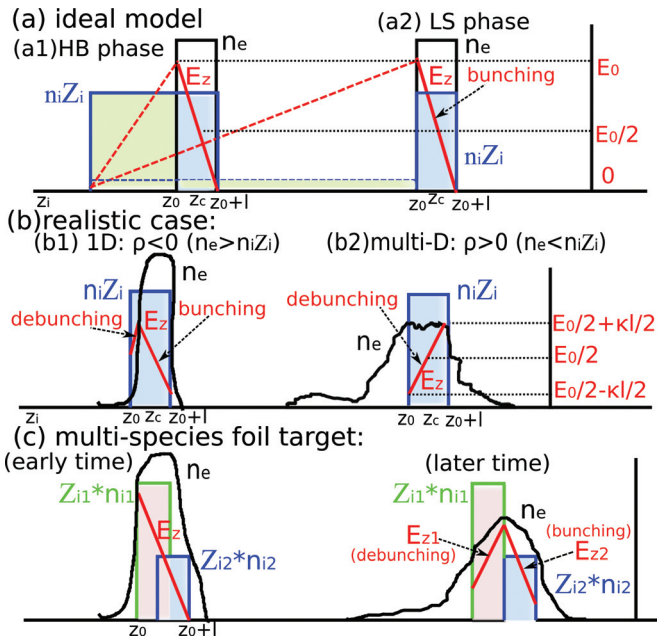

FIG. 1. (Color online) Schematic profiles of electron density (n_e, black), ion charge density (n_i Z_i, blue and green), and electrostatic field (E_z, red) for RPA cases of (a) ideal model, (b1) 1D simulations where the electron layer decompresses slowly, (b2) realistic multidimensional conditions where the electron layer decompresses rapidly, and (c) multispecies foil targets. Note here the main ion bunch is approximated as a uniform layer, ignoring the trailing particles.

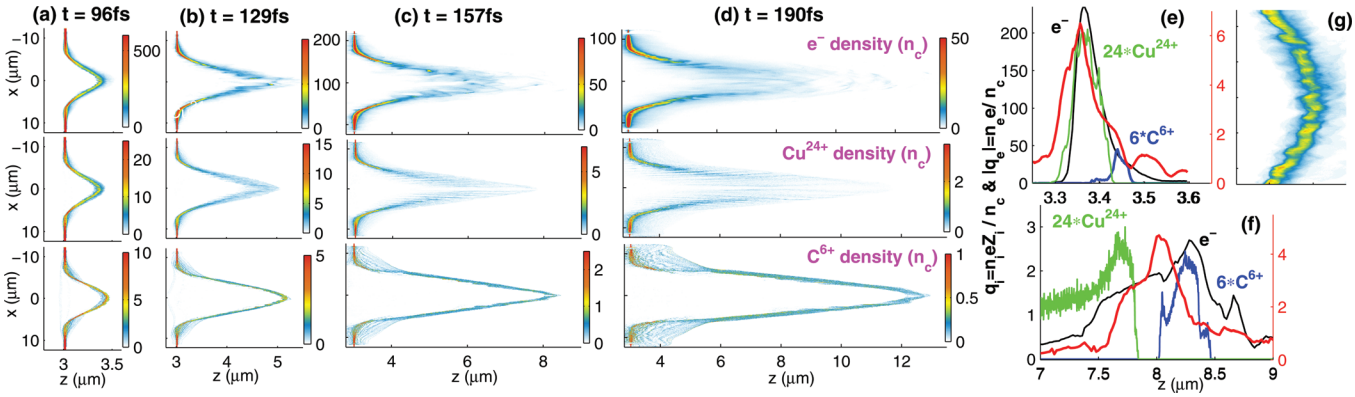

FIG. 2. (Color online) (a)–(d) Electron (e^-), Cu^{24+}, and C^{6+} densities at $t=96$, 129, 157, and 190fs for a 25 nm Cu–C-mixed foil irradiated by CP lasers at $I_0 = 5\times10^{20}$ W/cm^2. The density ratio is n_{i1}: $n_{i2}=5$:2 n_c, where $i1=\mathrm{Cu}^{24+}$ and $i2=\mathrm{C}^{6+}$. (e), (f) The corresponding longitudinal profiles and E_z [the red/gray line (with no labels)] cut at $x=0$ for (a) and (c), respectively. (g) The partially zoomed map of electron density at $t=105$fs, showing the instability initially happens at the laser-facing surface with small modulations.

can easily exceed the thin plasma slab. The electron layer thus decompresses rapidly during acceleration. In particular, this decompression is much accelerated by the transverse instabilities. The instabilities occur at the laser-facing surface by lots of small density modulations, see Fig. 2(g), resulting in enhanced heating of the electrons when the modulated surface interacts with laser pulses. Consequently the local net charge around the entire ion layer soon becomes positive $(n_e < n_i Z_i)$ and E_z changes to a debunching profile $E_z = E_0/2 + \kappa(z_i - z_c)$, shown in Fig. 1(b2). Once this occurs, the plasma slab density drops very rapidly [Eq. (4b)] and becomes transparent to the laser leading to premature termination of RPA.

From the above theoretical model, it becomes clear that the key condition for stable ion RPA is that the accelerating ion beam should remain accompanied with enough co-moving electrons to preserve a local bunching electrostatic field during the acceleration. As mentioned in the introduction, ion beam quasistable acceleration can be found at ultrahigh intensities $\geq 10^{22}$ W/cm^2, when the plasma slab becomes relativistic rapidly suppressing the growth of the instabilities and for the cases where the acceleration profile is transversely uniform leading to reduced heating and decompression of the electrons (by tailoring the density or intensity distributions). However, for RPA using moderate (currently easily achievable) laser pulses, modifications of the transverse profiles are insufficient to maintain the bunching electrostatic field and RPA terminates early resulting in lower ion energies and broadened energy spectra.

B. Possible scheme to achieve stable RPA

Because decompression of the co-moving electron layer for ion LS RPA by moderate laser pulses is unavoidable in the more realistic multidimensional case, one must find a way to supply enough additional electrons to the ion beam during acceleration for preserving the bunching structure of the electrostatic field E_z. One possible scheme is using a multispecies foil mixed with heavy and light ions. The core idea is described by Fig. 1(c), where the heavy ions have high-charge-state Z_{i1} and density n_{i1} while the light ions have lower Z_{i2} and n_{i2}, satisfying $Z_{i2} < Z_{i1}$ and $n_{i2}Z_{i2} < n_{i1}Z_{i1}$. At early times, the light ions are accelerated faster than the heavy ions due to larger charge-mass ratio and therefore are ahead of the latter. After the initial charge separation both heavy and light ions move together at the same velocity v_i due to space charge redistribution[15] because the electron layer is still stable initially. The light and heavy ion layers are accelerated together by the bunching E_z [see the left part of Fig. 1(c)], forming a whole plasma slab.

At later time when the electron layer decompresses heavily, the local net charge rapidly becomes positive $(n_{i1}Z_{i1} > n_e)$ around the heavy ion layer because the latter having higher-charge density needs more electrons for charge balance than the light ion layer. Consequently, the local electrostatic field changes to a debunching profile [E_{z1} in Fig. 1(c)] and the heavy ion layer debunches rapidly and becomes spectrally broadened. By contrast, the decompressed electron cloud from the heavy ions maintains a bunching electric field [E_{z2} in Fig. 1(c)] across the entire light ion layer as long as the latter's charge density is sufficiently low as $n_{i2}Z_{i2} < n_e$. The light ions maintain stable RPA due to the expanded electron charge cloud from the heavy ions. Therefore we expect the light ions to achieve efficient and stable RPA at moderate laser intensities.

III. 2D PIC SIMULATIONS

A. Stable RPA of C^{6+} beam by using Cu–C-mixed foils

To verify the theory, 2D PIC simulations have been run with the code "ILLUMINATION."[16] We choose a CP laser pulse with intensity $I_0 = 5\times10^{20}$ W/cm^2, wavelength $\lambda = 0.80$ μm, focus Gaussian radius $r_0 = 5$ μm, which can be easily achieved by current day lasers. The laser pulse has a temporal profile of first half Gaussian (FWHM duration 35fs) and second half flattop from $I(t)=I_0$, in order to be easily compared to both theory and more realistic experimental conditions. A copper–cabon-mixed foil is taken and assumed being fully ionized as Cu^{24+} and C^{6+}, where the foil thickness is $l_0=25$ nm. The electron density is $n_{e0}=660$ n_c and the density ratio of Cu^{24+} to C^{6+} is 5:2. In the simulations, 8000 cells along the laser axis of z-direction and 3072 cells transversely along x-axis constitute a 16×24.576 μm

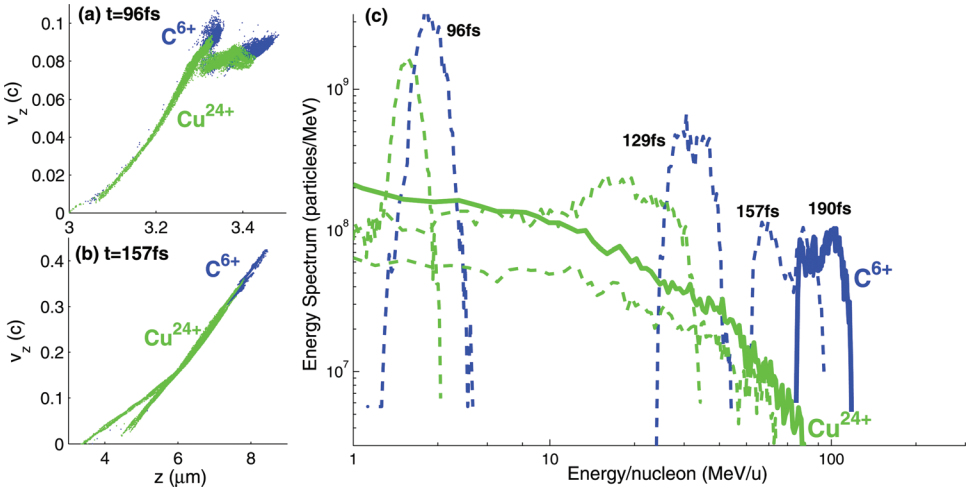

FIG. 3. (Color online) The phase space distributions of Cu^{24+} and C^{6+} at $t = 96$ (a) and 157fs (b) for those in Fig. 2 of the particles near the laser axis in the region $-3\ \mu m < x < 3\ \mu m$. Their energy spectra at different times are shown in (c), where the laser pulse has completely ended at $t = 190$fs.

simulation space. Each cell of the foil is filled up with 7000 quasiparticles in total.

Figures 2(a)–2(d) show density maps of electrons, Cu^{24+} and C^{6+} ions at time $t = 96$, 129, 157, and 190fs. At early time—Fig. 2(a)—we see the typical LS RPA image: both Cu^{24+} and C^{6+} layers and the electron layer are synchronously accelerated by radiation pressure, forming a negatively charged plasma slab. The motion of the slab obeys:[6,8]

$$\frac{dp}{dt} = \frac{2I}{\sum_i n_i m_i l_i c^2} \frac{\sqrt{1+p^2}-p}{\sqrt{1+p^2}+p}, \tag{5}$$

where n_i, m_i and l_i are density, mass, and thickness, respectively, of Cu^{24++} and C^{6+} ions for those of only the slab instead of the whole initial foil. $p = P/\sum_i m_i c$ is the normalized momentum. As shown in Fig. 2(e), the C^{6+} layer having larger charge-mass ratio moves ahead of the Cu^{24+} layer and both of them are synchronously accelerated by the bunching profile of E_z [the red/gray line (with no labels) in Fig. 2(e)], in consistence with the above theoretical model.

However, at later time, as shown in Figs. 2(b)–2(d), the electron layer decompresses rapidly, leading to complete separation of the Cu^{24+} and C^{6+} layers. As we expected, the Cu^{24+} layer has insufficient co-moving electrons [see Figs. 2(f), $24 \times n_{i1} > n_e$, $i1 = Cu^{24+}$] and thus undergoes rapid decompression [Figs. 2(c) and 2(d)] as the local E_z acquires a debunching profile. By contrast, the C^{6+} layer remains surrounded by excess co-moving electrons [Fig. 2(f), $6 \times n_{i2} < n_e$, $i2 = C^{6+}$] because of a large supplement from the decompressed electron cloud associated with the Cu^{24+} layer. The local negative net charge preserves a bunching profile of E_z [Fig. 2(f)] and stable RPA of the C^{6+} beam. This acceleration process agrees well with our theoretical expectations in Fig. 1(c).

Figures 3(a) and 3(b) plot the phase space distributions of Cu^{24+} and C^{6+} at two typical times $t = 96$ and 157fs for the particles near the laser axis in the region of $-3\ \mu m < x < 3\ \mu m$. We see from Fig. 3(a) that initially both phase spaces show a distinct concentrated head, further confirming that initially both Cu^{24+} and C^{6+} undergo synchronous RPA. Their energy spectra are given in Fig. 3(c), both showing obvious peaks. At later time—Fig. 3(b)—Cu^{24+} phase evolves into a long tail due to debunching, while C^{6+} phase space remains a distinct concentration. Correspondingly, Cu^{24+} energy spectrum is much broadened with no peak finally, while C^{6+} finally remains the well pronounced peak spectrum till the laser pulse has completely ended at $t = 190$fs, seen in Fig. 3(c). From Fig. 3(c) (the solid blue/dark line) we see that high-energy high-density quasimonoenergetic C^{6+} beam are obtained. The beam has a peak energy of 100 MeV/u and particle number about 10^9. Such high-quality C^{6+} ion beams have not been obtained by any other schemes at the same moderate laser intensities. We notice that a recent paper[13] has shown GeV light ion (proton) beam production from a double-layer foil target; however, there an ultraintense laser pulse at intensity of 3.9×10^{22} W/cm^2 is also used, as mentioned in the introduction.

The blue/dark (with cross markers) line in Fig. 4 shows the variation with time of the peak energy of C^{6+} beam from $t = 32.5$T ($T = 2\pi/\omega$). We can see clearly that the peak C^{6+} energy at later time scales as $t^{1/3}$, consistent with the typical analytical scaling (the red line with no markers) of the RPA scheme, Eq. (5). This proves that the C^{6+} beam in our simulation does experience stable RPA rather than the direct

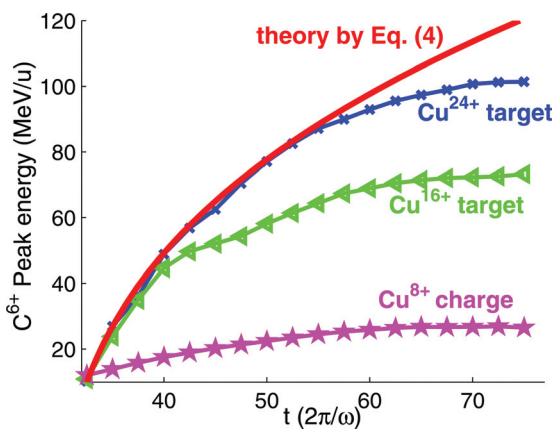

FIG. 4. (Color online) The evolutions in time of C^{6+} peak energy for Cu–C-mixed foils with Cu ionized states, respectively, of Cu^{24+}, Cu^{16+}, and Cu^{8+} from $t = 32.5$T which is the approximate transition point of their acceleration from HB to LS phases (when the distinct head in phase space has formed). The red line (with no markers) is the solution of Eq. (4), where n_i and l_i are estimated from the simulation at $t = 32.5$T.

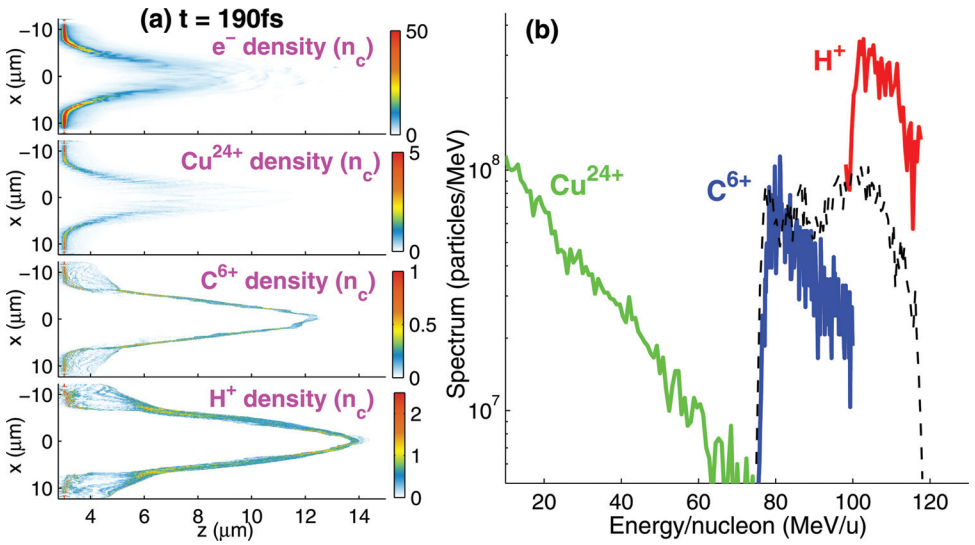

FIG. 5. (Color online) The densities (a) and energy spectra (b) of all species at $t = 190$fs when the laser pulse ends for the three-species ($Cu–CH_6$) foil case, where the dashed line is that of C^{6+} in Fig. 3(c) (the solid blue/dark line). The total mass densities and other parameters are the same as Fig. 2.

Coulomb explosion (DCE).[17] As a matter of fact, the DCE scheme has been proposed for the case of linearly polarized lasers, and there the intensity must be extremely high of 2.7×10^{22} W/cm^2 so that almost all electrons are blown out and the ion core is accelerated by Coulomb explosion, i.e., $a_0 \geq \pi(n_{e0}/n_c)(l_0/\lambda)$, being contrary to the equilibrium condition of RPA scheme.[2,8] Moreover, the concentration of phase space distribution in the above Fig. 3 can not be seen in the DCE scheme because there most of the electrons are blown out and the local charge density is positive [see Fig. 5(a) in the paper of Bulanov *et al.*[17]].

In order to further confirm the key condition for stable RPA obtained above, PIC simulations for Cu–C-mixed foils with lower (not fully) Cu ionized states $Z_{i1} = 16+$ and $8+$ have also been run, where the mass densities are the same as above. Figure 4 also gives the evolutions in time of C^{6+} peak energy for these two cases. We see clearly that the acceleration of C^{6+} beam is more stable for the cases of Cu species with higher-charge state Z_{i1}, because higher Z_{i1} means more electrons can be supplied to stabilize C^{6+} acceleration. On the other hand, we can see that above 50 MeV/u monoenergetic C^{6+} beam can still be obtained even if the target is only half ionized to Cu^{16+}.

B. Stable RPA of C^{6+} and proton beams by using $Cu–CH_6$-mixed foils

The above scheme also applies to three-species foil target case. We choose a Cu foil contaminated with CH_6 impurities irradiated by the same CP laser pulse and assumed it being fully ionized as Cu^{24+}, C^{6+}, and H^+, which are closer to the experimental conditions. The mass densities of the whole foil and the Cu^{24+} species are both kept the same as those above. Figures 5(a) and 5(b) show that high-energy monoenergetic C^{6+} beam and H^+ (proton) beam are both obtained at $t = 190$fs when the laser pulse ends. The C^{6+} beam has a peak energy of about 90 MeV/u, density 0.2 n_c and particle number of 5×10^8, while the proton beam has a peak energy of 110 MeV/u, density 1.0 n_c and particle number of 10^9. The comparison of their energy spectra with that of C^{6+} in the above two-species case [the dashed line in Fig. 5(b)] further confirms the RPA dynamics of Eq. (5), i.e., the acceleration depends on the total mass density of the slab. Note that here the peak energies of the ion beams are limited by the laser energy. If a higher-energy laser with either longer pulse or higher intensity can be arrived, one can obtain much higher-energy ion beams.

IV. SUMMARY

To summarize, we have identified the key condition for efficient and stable ion RPA from thin foils by CP laser pulses at moderate intensities via theoretical modeling and PIC simulations. That is, the ion beam should remain accompanied with enough co-moving electrons to preserve a local bunching electrostatic field during the acceleration. In realistic LS RPA regime, the decompression of the co-moving electron layer leads to a change of local electrostatic field from a bunching to a debunching profile, resulting in premature termination of ion beam acceleration. One possible scheme to achieve stable RPA is using a multispecies foil. In the scheme, the lower-Z ion species acquire large supplementary electrons from those associated with the high-Z ion species, preserving stable RPA. Two-dimensional PIC simulations show that 100 MeV/u monoenergetic C^{6+} beam are produced by irradiation of a Cu–C-mixed foil with CP lasers at intensities of 5×10^{20} W/cm^2, easily achievable by current day lasers. Note that the scheme also works with multispecies foil target of other finite-Z ions as long as the conditions $Z_{i2} < Z_{i1}$ and $n_{i2}Z_{i2} < n_{i1}Z_{i1}$ are satisfied. More realistic three-dimensional PIC simulations are planed on larger supercomputers to confirm the theory in the near future.

ACKNOWLEDGMENTS

B.Q. acknowledges the support from the Alexander von Humboldt Foundation. M.Z. thanks the support from the Royal Society. The work was also supported by EPSRC (Grant Nos. EP/C003586/1 and EP/D/06337X/1). Computing resources on JUROPA at JSC (Grant Nos. jzam04 and jjsc04) and VIP at RZG (collaboration grant with MPQ) are both acknowledged.

[1]E. L. Clark, K. Krushelnick, J. R. Davies, M. Zepf, M. Tatarakis, F. N. Beg, A. Machacek, P. A. Norreys, M. I. K. Santala, I. Watts, and A. E. Dangor, Phys. Rev. Lett. **84**, 670 (2000); A. Maksimchuk, S. Gu, K. Flippo, D. Umstadter, and V. Yu. Bychenkov, *ibid*. **84**, 4108 (2000); R. A. Snavely, M. H. Key, S. P. Hatchett, T. E. Cowan, M. Roth, T. W. Phillips, M. A. Stoyer, E. A. Henry, T. C. Sangster, M. S. Singh, S. C. Wilks, A. MacKinnon, A. Offenberger, D. M. Pennington, K. Yasuike, A. B. Langdon, B. F. Lasinski, J. Johnson, M. D. Perry, and E. M. Campbell, *ibid*. **85**, 2945 (2000).
[2]T. Esirkepov, M. Borghesi, S. V. Bulanov, G. Mourou, and T. Tajima, Phys. Rev. Lett. **92**, 175003 (2004).
[3]A. Macchi, F. Cattani, T. V. Liseykina, and F. Cornolt, Phys. Rev. Lett. **94**, 165003 (2005).
[4]B. M. Hegelich, B. J. Albright, J. Cobble, K. Flippo, S. Letzring, M. Paffett, H. Ruhl, J. Schreiber, R. K. Schulze, and J. C. Fernandez, Nature (London) **439**, 441 (2006).
[5]M. Borghesi, J. Fuchs, S. V. Bulanov, A. J. MacKinnon, P. K. Patel, and M. Roth, Fusion Sci. Technol. **49**, 412 (2006).
[6]A. P. L. Robinson, M. Zepf, S. Kar, R. G. Evans, and C. Bellei, New. J. Phys. **10**, 013021 (2008).
[7]X. Q. Yan, C. Lin, Z. M. Sheng, Z. Y. Guo, B. C. Liu, Y. R. Lu, J. X. Fang, and J. E. Chen, Phys. Rev. Lett. **100**, 135003 (2008).
[8]B. Qiao, M. Zepf, M. Borghesi, and M. Geissler, Phys. Rev. Lett. **102**, 145002 (2009).
[9]B. Qiao, P. Gibbon, M. Zepf, M. Borghesi, A. Karmakar, and M. Geissler, Phys. Rev. Lett. **105**, 155002 (2010).
[10]F. Pegoraro and S. V. Bulanov, Phys. Rev. Lett. **99**, 065002 (2007).
[11]M. Chen, A. Pukhov, Z. M. Sheng, and X. Q. Yan, Phys. Plasmas **15**, 113103 (2008); M. Chen, A. Pukhov, T. P. Yu, and Z. M. Sheng, Phys. Rev. Lett. **103**, 024801 (2009).
[12]T. P. Yu, A. Pukhov, G. Shvets, and M. Chen, Phys. Rev. Lett. **105**, 065002 (2010).
[13]Z. M. Zhang, X. T. He, Z. M. Sheng, and M. Y. Yu, Phys. Plasmas **18**, 023110 (2011).
[14]A. Macchi, S. Veghini, and F. Pegoraro, Phys. Rev. Lett. **103**, 085003 (2009).
[15]A. P. L. Robinson, P. Gibbon, M. Zepf, S. Kar, R. G. Evans, and C. Bellei, Plasma Phys. Controlled Fusion **51**, 024004 (2009); A. P. L. Robinson, D.-H. Kwon, and K. Lancaster, *ibid*. **51**, 095006 (2009).
[16]M. Geisser, J. Schreiber, and J. Meyer-ter-Vehn, New. J. Phys. **8**, 186 (2006); M. Geissler, S. Rykovanov, J. Schreiber, J. Meyer-ter-Vehn, and G. D. Tsakiris, *ibid*. **9**, 218 (2007).
[17]S. S. Bulanov, A. Brantov, V. Yu. Bychenkov, V. Chvykov, G. Kalinchenko, T. Matsuoka, P. Rousseau, S. Reed, V. Yanovsky, D. W. Litzenberg, K. Krushelnick, and A. Maksimchuk, Phys. Rev. E **78**, 026412 (2008).